NASA TECHNICAL NOTE

NASA TN D-2429




NASA TN D-2429

# ANALYTICAL INVESTIGATION OF THE RADIATOR AREA CHARACTERISTICS OF OUT-OF-PILE THERMIONIC GAS CYCLE SPACE POWER SYSTEMS

*by Michael R. Vanco and Arthur J. Glassman*

*Lewis Research Center*

*Cleveland, Ohio*

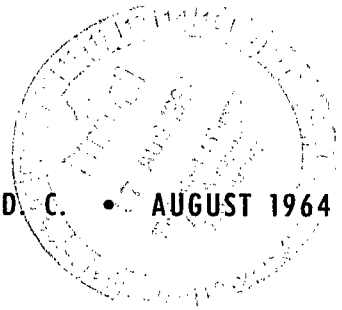

NATIONAL AERONAUTICS AND SPACE ADMINISTRATION • WASHINGTON, D. C. • AUGUST 1964

# ANALYTICAL INVESTIGATION OF THE RADIATOR AREA CHARACTERISTICS OF OUT-OF-PILE THERMIONIC GAS CYCLE SPACE POWER SYSTEMS

By Michael R. Vanco and Arthur J. Glassman

Lewis Research Center
Cleveland, Ohio

NATIONAL AERONAUTICS AND SPACE ADMINISTRATION

For sale by the Office of Technical Services, Department of Commerce,
Washington, D.C. 20230 -- Price $1.00

# ANALYTICAL INVESTIGATION OF THE RADIATOR AREA CHARACTERISTICS OF OUT-OF-PILE THERMIONIC GAS CYCLE SPACE POWER SYSTEMS

by Michael R. Vanco and Arthur J. Glassman

Lewis Research Center

## SUMMARY

The radiator area potential of out-of-pile thermionic space power systems using an inert gas as the heat-transfer medium was assessed by studying the radiator area characteristics of three typical cycles and comparing the minimum radiator area requirements with those for a turboelectric Brayton cycle. The three cycles considered were the Split Radiator, the Two Loop, and the Turbineless cycles. This study was primarily a thermodynamic cycle analysis, with thermionic converter efficiency being treated both parametrically and through the use of experimental data.

On the basis of this thermodynamic analysis, no significant difference in radiator area requirements was found among the three out-of-pile thermionic gas cycles. A comparison of radiator area requirements for one of these cycles with those for a turboelectric Brayton cycle showed that either high converter efficiencies or high converter inlet temperatures are necessary if an out-of-pile thermionic gas cycle is to have any radiator area advantage over the Brayton cycle. Converter efficiencies greater than about 0.3 of Carnot or converter inlet temperatures greater than 3500° R are required to make the out-of-pile thermionic gas cycle appear attractive.

## INTRODUCTION

The electric rocket is one of the propulsion systems considered for interplanetary space missions. Power levels for electric rockets will range from several hundred kilowatts for unmanned probes to many megawatts for manned expeditions. Electric propulsion systems will require powerplants that have low specific weights (powerplant weight/power output) because the electric rocket's potential advantage over other modes of propulsion increases as powerplant specific weight decreases (ref. 1). At the power levels of interest for interplanetary missions, the major obstacle to the achievement of low specific weight is the large radiator required for the powerplant.

The necessary quantities of electric power can be generated either indi-

rectly (turboelectric cycle) or directly from the system heat supply. One of the direct energy-conversion methods under consideration is the thermionic conversion system (refs. 1 to 3). Thermionic conversion systems have the potential for operating with higher temperature levels than turboelectric systems can and, thereby, may be able to achieve a considerable reduction in radiator size (refs. 2 and 3).

Recently, there has been renewed interest in space power systems using gaseous fluids. The noncorrosive, nonerosive character of inert gases gives such systems the potential of being extremely reliable. An analytical study (ref. 2) of radiator area requirements for thermionic gas cycle systems as well as Brayton cycle systems has indicated that the in-pile (diodes in reactor) system requires the smallest radiator. An out-of-pile (diodes in radiator or heat exchanger) system, however, appears to represent a more easily achievable system because of the location of the diodes away from the reactor core.

In view of a possible interest in out-of-pile thermionic gas systems for space power applications, an analytical investigation was conducted in order to supplement a previous study (ref. 2) and better assess the radiator area potential of these systems. This was accomplished by studying the radiator area characteristics of three typical out-of-pile systems and comparing minimum radiator requirements with those for a turboelectric Brayton cycle. The detailed variation of radiator areas as a function of the many variables and parameters is presented for only one of the cycles studied in order to illustrate the pertinent effects, which are similar for all three cycles. The minimum radiator area requirements for all three cycles are then presented and the desired comparisons are made.

## SYMBOLS

$A$ radiator area, sq ft

$c_p$ specific heat, Btu/(lb)($^\circ$R)

$D$ cathode-to-anode temperature difference, $^\circ$R

$E$ recuperator effectiveness

$\Delta h$ enthalpy change, Btu/hr

$h_R$ radiator gas heat-transfer coefficient, Btu/(hr)(sq ft radiator area)($^\circ$R)

$P$ electric power output, kw

$p$ absolute pressure, psia

$Q_s$ heat supplied to cathode, Btu/hr

$R$ pressure ratio

$T$ absolute temperature, $^{\circ}R$

$w$ weight flow, lb/hr

$\gamma$ specific heat ratio

$\epsilon$ emissivity

$\eta$ efficiency

$\theta$ ratio of gas temperature to cathode temperature

$\sigma$ Stefan-Boltzmann constant, $0.173 \times 10^{-8}$ Btu/(hr)(sq ft)($^{\circ}R^4$)

$\psi$ ratio of actual to Carnot converter efficiency

Subscripts:

a anode

av average

C compressor

c cathode

cy cycle

g gas

HT high temperature

i ideal

jk ratio of variable value at point j to variable value at point k for j, k = 1, 2, . . ., 9

L loss

LT low temperature

m motor

min minimum

n net

opt optimum

P primary radiator

S secondary radiator

| | |
|---|---|
| s | sink |
| T | turbine |
| th | thermionic converter |
| tot | total |
| w | wall |
| I,II | loops I and II, Two Loop cycle |
| 1 to 9 | state points defined by fig. 1, 2, or 3 |

## DESCRIPTION OF CYCLES

In order to study out-of-pile thermionic gas cycle radiator area requirements, three typical cycles were chosen for the investigation. These three cycles are designated as (1) the Split Radiator cycle (ref. 2), (2) the Two Loop cycle, and (3) the Turbineless cycle. Undoubtedly, with some imagination, other cycles can be conceived; this study, however, is restricted to the three basic cycles mentioned. A detailed description of each of these cycles follows. Hybrid cycles (i.e., those producing both thermionic and turboelectric power) were not considered in this analysis.

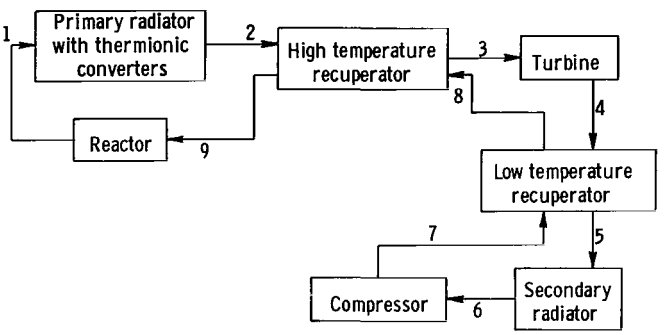


(a) Schematic diagram.

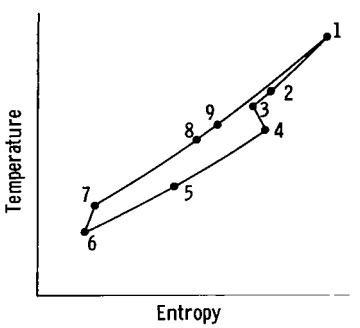


(b) Temperature-entropy diagram.

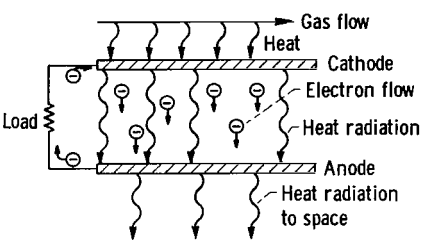


(c) Converter representation.

Figure 1. - Split Radiator thermionic gas cycle.

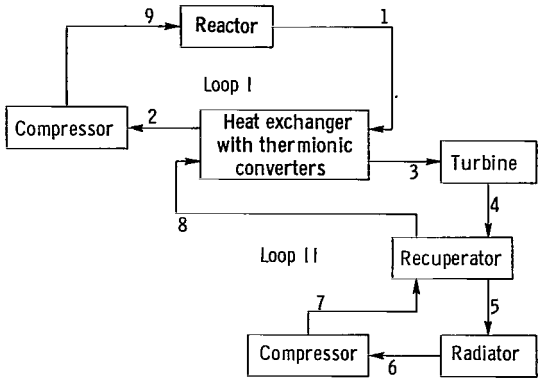


(a) Schematic diagram.

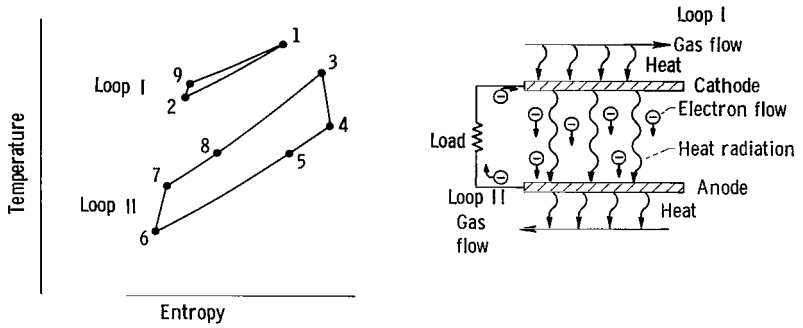


(b) Temperature-entropy diagram.

(c) Converter representation.

Figure 2. - Two loop thermionic gas cycle.

## Split Radiator Cycle

A schematic diagram of the Split Radiator cycle is presented in figure 1(a), and the corresponding temperature-entropy diagram is presented in figure 1(b). The hot gas (point 1) from the reactor enters the primary radiator, which contains the thermionic diodes, where it is cooled (to point 2) by transferring heat to the cathode elements. A portion of this heat is converted to electricity, and the remainder is transferred to the anodes and rejected to space by radiation. A simplified representation of the converter is shown in figure 1(c). Leaving the primary radiator, the gas enters the high temperature recuperator and is cooled (to point 3) as it transfers heat to the gas coming from the low temperature recuperator. In the turbine, the gas expands (to point 4), producing the work required to drive the compressor. The gas then enters the low temperature recuperator and is cooled (to point 5) by transferring heat to gas coming from the compressor. Final cooling of the gas (to point 6) occurs in the secondary radiator. The gas is then compressed (to point 7), heated (to point 8) in the low temperature recuperator, further heated (to point 9) in the high temperature recuperator, and finally heated to its maximum temperature (point 1) in the reactor.

## Two Loop Cycle

The Two Loop cycle is shown schematically in figure 2(a) and thermodynamically in figure 2(b). The hot gas (point 1) from the reactor enters the heat exchanger, which contains the thermionic diodes, where it is cooled (to point 2) by transferring heat to the cathode elements. Upon leaving the heat exchanger, the hot loop gas is compressed (to point 9) and heated to its maximum temperature (point 1) in the reactor. In the heat exchanger, a portion of the heat is converted to electricity and the remainder is transferred to the anode and removed by the cold loop gas. A simplified representation of this converter is shown in figure 2(c). Leaving the heat exchanger, the cold loop gas (point 3) expands through the turbine, thus producing the work required to drive both compressors. The gas (point 4) then enters the recuperator and is cooled (to point 5) by transferring heat to the gas coming from the compressor. Final cooling of the gas (to point 6) occurs in the radiator, where the excess heat is rejected to space. The gas is then compressed (to point 7), heated (to point 8) in the recuperator, and returned to the heat exchanger.

## Turbineless Cycle

A schematic diagram of the Turbineless cycle is presented in figure 3(a), and the corresponding temperature-entropy diagram is presented in figure 3(b). The hot gas (point 1) from the reactor enters the radiator, which contains the

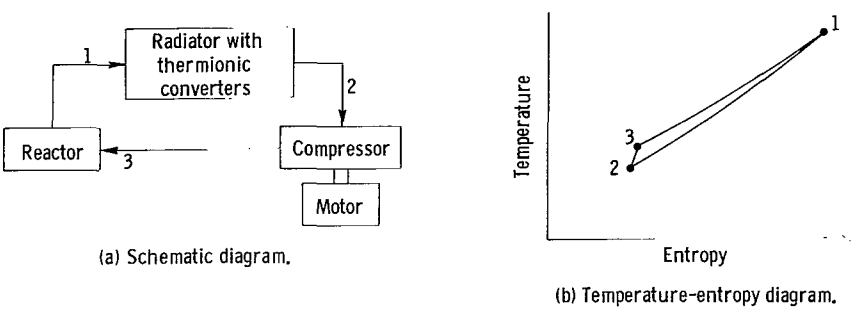


(a) Schematic diagram.

(b) Temperature-entropy diagram.

Figure 3. - Turbineless thermionic gas cycle.

thermionic diodes, where it is cooled (to point 2) by transferring heat to the cathode elements. A portion of this heat is converted to electricity, and the remainder is transferred to the anodes and rejected to space by radiation, as in the Split Radiator cycle. The gas is then compressed (to point 3) and returned to the reactor. A portion of the thermionic converter output is used to power the compressor motor.

## METHOD OF ANALYSIS

This analysis was conducted in two parts. First, a detailed investigation of radiator area requirements was made for each of the three cycles in order to determine the pertinent variables and parameters and optimize as many

of these as possible. The optimized cycles were then compared in order to determine whether any significant differences exist with respect to radiator area requirements. For this study, prime area was used as the indicator of radiator size. A prime area radiator can be defined as a radiator without fins Prime area is a commonly used and quite an accurate indicator of the relative size of actual radiators. The first part of the study, hereinafter referred to as the ideal analysis, was made on the basis of ideal heat transfer in the thermionic converter (no temperature difference between the gas and the diodes) and a parametric treatment of converter efficiency in terms of a percentage of Carnot efficiency.

The second part of the study consisted of a further analysis of one of the cycles studied in the ideal analysis and a comparison of the radiator area required for that cycle with the area required for a turboelectric Brayton cycle. The additional analysis of the selected cycle incorporates the use of experimental thermionic converter efficiencies and a parametric treatment of the temperature ratio between the gas and the diodes.

## Ideal Analysis

The pertinent equations that must be derived for the three cycles being studied are those for the evaluation of radiator area. In order to compute radiator area, it is necessary for thermionic converter efficiency, fluid specific capacity rate ($wc_p/P$), and certain cycle temperatures to be specified in terms of the cycle variables and parameters. In addition, cycle efficiency is of general interest for any cycle. Mention has been made of cycle variables and cycle parameters. For the purposes of this study, the cycle variables are defined as the ratios of temperatures or pressures that can be varied independently in order to optimize the cycle. The cycle parameters are defined as those quantities that should be as high or as low as possible (e.g., turbomachinery efficiency, pressure drop, temperature level) but are subject to practical limitations (e.g., achievable performance, component size, stress).

The efficiency, capacity rate, and temperature equations for the Split Radiator, Two Loop, and Turbineless cycles are derived in appendixes A, B, and C, respectively, for use in the radiator area equations to be derived in this section. These derivations are made using the following assumptions:

(1) The working fluid is an ideal gas.

(2) There are no heat losses or mechanical losses.

(3) The ratio of actual to Carnot converter efficiency is constant for any given system.

(4) Gas temperature is equal to diode temperature.

(5) The temperature differences across all metal walls are negligible.

(6) Heat conduction along any tube axis is neglected.

(7) Sink temperature is constant for any given radiator.

(8) For radiator-mounted diodes, the temperature difference between cathode and anode is constant.

Split Radiator cycle. - There are two radiators in this cycle: the primary radiator, which contains the thermionic diodes, and the secondary radiator. For any differential element of tube length in the primary radiator, the heat lost by the gas and not converted to electricity must be equal to the heat that is radiated to space

$$-(1 - \eta_{th})wc_p \, dT_g = \sigma\epsilon(T_a^4 - T_s^4) \, dA_P \tag{1}$$

Substituting $\psi D/T_c$ for $\eta_{th}$ (eqs. (A1) and (A3)), $dT_c$ for $dT_g$ (since $T_c = T_g$), and $T_c - D$ for $T_a$ yields, after rearrangement,

$$-\frac{dT_c}{(T_c - D)^4 - T_s^4} + \frac{\psi D \, dT_c}{T_c\left[(T_c - D)^4 - T_s^4\right]} = \frac{\sigma\epsilon}{wc_p} \, dA_P \tag{2}$$

Equation (2) can be integrated by the method of partial fractions. Integrating between the limits of 0 to $A_P$ and $T_1$ to $T_2$ and dividing both sides by P yield

$$\frac{A_P}{P} = \left(\frac{wc_p}{P}\right)\left(\frac{1}{\sigma\epsilon}\right)\left[\frac{\psi D}{T_s^4 - D^4} \ln \frac{T_1}{T_2} + \frac{1}{4T_s^3}\left(1 - \frac{\psi D}{T_s + D}\right)\ln \frac{T_1 - D - T_s}{T_2 - D - T_s}\right.$$

$$- \frac{1}{4T_s^3}\left(1 + \frac{\psi D}{T_s - D}\right) \ln \frac{T_1 - D + T_s}{T_2 - D + T_s} - \frac{\psi D}{4T_s^2(T_s^2 + D^2)} \ln \frac{(T_1 - D)^2 + T_s^2}{(T_2 - D)^2 + T_s^2}$$

$$\left. + \frac{1}{2T_s^3}\left(1 - \frac{\psi D^2}{T_s^2 + D^2}\right)\left(\arctan \frac{T_2 - D}{T_s} - \arctan \frac{T_1 - D}{T_s}\right)\right] \tag{3}$$

where $wc_p/P$ is obtained from equation (A7).

For any differential element of tube length in the secondary radiator, the heat transferred from the fluid to the tube wall must equal the heat radiated to space, that is,

$$h_R(T - T_w)dA_s = \sigma\epsilon(T_w^4 - T_s^4)dA_s \tag{4a}$$

Rearrangement of equation (4a) results in

$$T = T_w + \frac{\sigma\epsilon}{h_R}(T_w^4 - T_s^4) \tag{4b}$$

The decrease in fluid sensible heat must also equal the heat radiated. Thus,

$$-wc_p\,dT = \sigma\epsilon(T_w^4 - T_s^4)dA_S \tag{5}$$

Differentiation of equation (4b), substitution of the differentiated expression into equation (5), and rearrangement give

$$dA_S = -wc_p\left[\frac{4T_w^3}{h_R(T_w^4 - T_s^4)} + \frac{1}{\sigma\epsilon(T_w^4 - T_s^4)}\right]dT_w \tag{6}$$

Integrating equation (6) by the method of partial fractions between the limits of 0 to $A_S$ and $T_{w,5}$ to $T_{w,6}$ and dividing by P yield

$$\frac{A_S}{P} = \left(\frac{wc_p}{P}\right)\left\{\frac{1}{h_R}\ln\frac{T_{w,5}^4 - T_s^4}{T_{w,6}^4 - T_s^4} + \frac{1}{4\sigma\epsilon T_s^3}\left[\ln\frac{(T_{w,5} - T_s)(T_{w,6} + T_s)}{(T_{w,6} - T_s)(T_{w,5} + T_s)} - 2\left(\arctan\frac{T_{w,5}}{T_s} - \arctan\frac{T_{w,6}}{T_s}\right)\right]\right\} \tag{7}$$

where $T_w$ is related to T by equation (4b) and $wc_p/P$ is obtained from equation (A7).

Total radiator area for the Split Radiator cycle, therefore, is

$$\frac{A_{tot}}{P} = \frac{A_P}{P} + \frac{A_S}{P} \tag{8}$$

Two Loop cycle. - The radiator for this cycle is similar in nature to the secondary radiator in the Split Radiator cycle. Total radiator area for the Two Loop cycle, consequently, can be computed from equation (7) with the exception that fluid specific capacity rate for this cycle is equal to $w_{II}c_p/P$, which is evaluated from equation (B7).

Turbineless cycle. - The radiator for this cycle is similar in nature to the primary radiator in the Split Radiator cycle. Total radiator area for the Turbineless cycle, consequently, can be computed from equation (3) with the exception that fluid specific capacity rate for this cycle is equal to $wc_p/P_n$, which is evaluated from equation (C3).

## Nonideal Considerations

The nonideal considerations of a gas-to-diode temperature difference and experimentally determined converter efficiencies were applied only to the Split Radiator cycle in order to illustrate the effects of these considerations.

Gas-to-diode temperature difference. - The temperature difference between

the gas and the cathode is expressed as the ratio of gas temperature to cathode temperature

$$\theta = \frac{T_g}{T_c} \tag{9}$$

Modification of the Split Radiator cycle analysis to include the effect of this temperature ratio is as follows. Substituting equation (9) into equation (A3) and integrating equation (A2b) from $T_g = T_1$ to $T_g = T_2$ show that

$$\eta_{th,i,av} = \theta(\eta_{th,i,av})_{\text{ideal heat transfer}} \tag{10}$$

Making this substitution into equation (A6) shows

$$\frac{wc_p}{P} = \frac{1}{\theta}\left(\frac{wc_p}{P}\right)_{\text{ideal heat transfer}} \tag{11}$$

The required radiator area for this cycle also is affected by the temperature ratio $\theta$. Setting $dT_c = dT_g$ and $T_c = T_g/\theta$ in equation (2) yields

$$\frac{A_P}{P} = \left(\frac{wc_p}{P}\right)\left(\frac{\theta}{\sigma\epsilon}\right)\left[\frac{\psi D}{T_s^4 - D^4}\ln\frac{T_1}{T_2} + \frac{1}{4T_s^3}\left(1 - \frac{\psi D}{T_s + D}\right)\ln\frac{\frac{T_1}{\theta} - D - T_s}{\frac{T_2}{\theta} - D - T_s}\right.$$

$$- \frac{1}{4T_s^3}\left(1 + \frac{\psi D}{T_s - D}\right)\ln\frac{\frac{T_1}{\theta} - D + T_s}{\frac{T_2}{\theta} - D + T_s} - \frac{\psi D}{4T_s^2(T_s^2 + D^2)}\ln\frac{\left(\frac{T_1}{\theta} - D\right)^2 + T_s^2}{\left(\frac{T_2}{\theta} - D\right)^2 + T_s^2}$$

$$\left. + \frac{1}{2T_s^3}\left(1 - \frac{\psi D^2}{T_s^2 + D^2}\right)\left(\arctan\frac{\frac{T_2}{\theta} - D}{T_s} - \arctan\frac{\frac{T_1}{\theta} - D}{T_s}\right)\right] \tag{12}$$

where $wc_p/P$ is obtained from equation (11). The only change required for the secondary radiator area, equation (7), is that $wc_p/P$ be obtained from equation (11). It can be seen from these modifications that setting $\theta = 1$ reduces the equations to those for the case of the ideal analysis.

Experimental converter efficiencies. - Since experimentally-determined converter efficiencies are available in the published literature, it was felt that their use would strengthen the analysis and especially the comparison of thermionic cycle radiator area with Brayton cycle radiator area. Two sources of experimental data, references 4 and 5, were selected for this analysis. These data are believed to represent state-of-the-art efficiency levels for laboratory-scale converters. The experimental data from references 4 and 5 are presented in the form of efficiency against cathode temperature in figure 4(a)

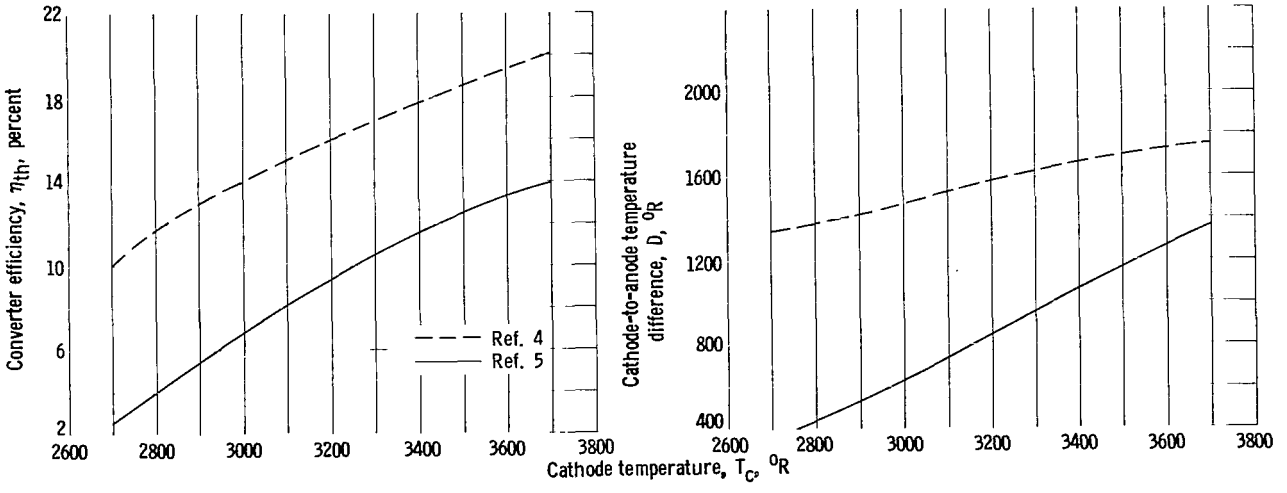


(a) Efficiency.

(b) Cathode-to-anode temperature difference.

Figure 4. - Experimental converter performance.

and cathode-to-anode temperature difference against cathode temperature in figure 4(b). These data were used in the analysis by first computing average values for converter efficiency and cathode-to-anode temperature difference for each cycle operating point and then using the previously derived equations.

## RESULTS OF ANALYSIS

To show the complete parametric results of the detailed ideal analyses for all three cycles studied would result in an excessive and unnecessary number of curves. In order to show the manner in which the cycle variables are optimized to yield minimum radiator area and to show the effects of the design parameters on radiator area, detailed results will be presented for the Split Radiator cycle. The optimization philosophy and the general effects of the parameters are similar for the other two cycles of interest. The minimum radiator areas for all three cycles will then be presented. Finally, the radiator area comparison with a turboelectric Brayton cycle will be made on the basis of both the ideal analysis and the nonideal considerations.

The radiator area studies and comparisons were made on the basis of typical design parameter values for each cycle. The selected design parameter values were those that are believed to be reasonable and/or represent achievable state-of-the-art capabilities. These parameter values are presented in the following table:

Design Parameters

| Parameter | Cycle value | | | |
|---|---|---|---|---|
| | Split Radiator | Two Loop | Turbine-less | Brayton (ref. 6) |
| Maximum cycle temperature, $T_1$, °R | 2000-4000 | 2000-4000 | 2000-4000 | 2000-4000 |
| Ratio of actual to Carnot converter efficiency, $\psi$ | 0.30 | 0.30 | 0.30 | --- |
| Turbine efficiency, $\eta_T$ | 0.85 | 0.85 | --- | 0.85 |
| Compressor efficiency, $\eta_C(\eta_{C,I}, \eta_{C,II})$ | 0.80 | (0.85, 0.80) | 0.85 | 0.80 |
| Loss pressure ratio, $R_L(R_{L,I}, R_{L,II})$ | 0.90 | (0.95, 0.90) | 0.95 | 0.90 |
| Effectiveness, $E(E_{LT}, E_{HT})$ | (0.85, 0) | 0 | --- | 0.85 |
| Emissivity, $\epsilon$ | 0.90 | 0.90 | 0.90 | 0.90 |
| Sink temperature, $T_s$, °R | 400 | 400 | 400 | 400 |
| Motor efficiency, $\eta_m$ | --- | --- | 0.80 | --- |
| Heat-transfer coefficient, $h_R$ | 50 | 50 | --- | 50 |
| Specific heat ratio, $\gamma$ | 1.667 | 1.667 | 1.667 | 1.667 |

In some cases a selected parameter value may differ for different cycles because of different compressor pressure ratios or a different number of pressure drop contributors. Since the pertinent parameters and their significances differ for the various cycles, it is impossible for any radiator area comparison to be on a strictly comparable basis; it is recognized, consequently, that small or even moderate differences in the computed radiator areas may not be truly significant.

## Split Radiator Cycle

The equations developed for the Split Radiator cycle show that total radiator area is a function of several design parameters and three independent variables (see appendix A and METHOD OF ANALYSIS). The manner in which the cycle variables affect radiator area is discussed first, and then the effects of the design parameter factors are explored. Except where otherwise indicated, the previously tabulated design parameter values, with the addition of a converter inlet temperature of 3000° R, were used for the example computations.

Radiator area is plotted against compressor pressure ratio in figure 5 for both the primary and secondary radiators, as well as for the sum of the two radiators. Primary radiator area is seen to be independent of pressure ratio as would be expected since equation (3) shows no pressure ratio dependence. Secondary radiator area decreases sharply with increasing pressure ratio in the low pressure ratio region but becomes relatively insensitive to further increases in pressure ratio. Although secondary radiator area passes through a minimum at a pressure ratio of about 1.6, the minimum is extremely

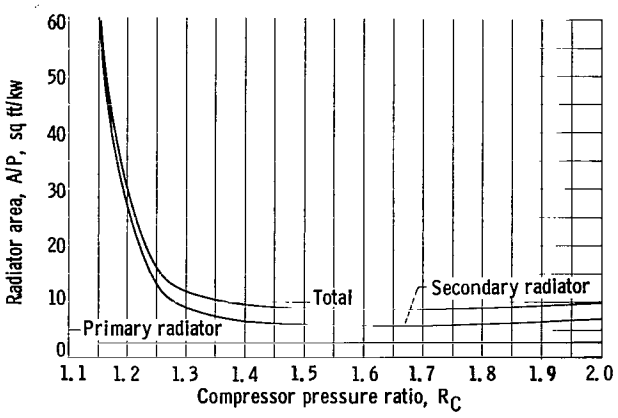


Figure 5. - Effect of compressor pressure ratio on primary and secondary radiator areas for Split Radiator cycle. Diode difference temperature ratio, 0.375; converter gas temperature ratio, 0.80.

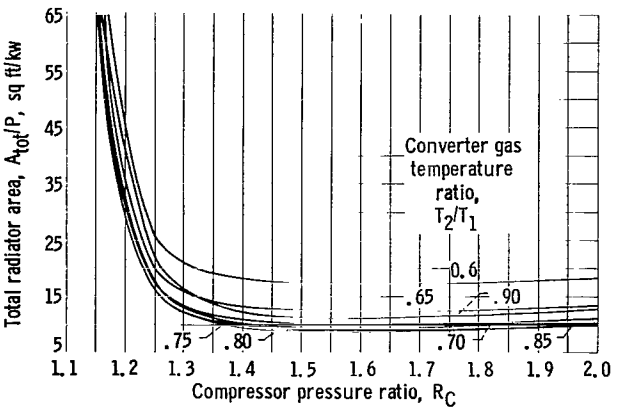


Figure 6. - Effect of converter gas temperature ratio and compressor pressure ratio on total radiator area for Split Radiator cycle. Diode difference temperature ratio, 0.375.

shallow and radiator area requirements do not change much in the pressure ratio range of about 1.4 to 2.0. Since primary radiator area is constant, total radiator area behaves in a manner similar to secondary radiator area.

Total radiator area is plotted against compressor pressure ratio in figure 6 for several values of the ratio of converter gas exit to gas inlet temperature, hereinafter called converter gas temperature ratio. As can be seen from this figure, the manner in which radiator area varies with pressure ratio, except for the magnitude of the area, is similar for all pertinent values of converter gas temperature ratio and, for all practical purposes, the minimum radiator area occurs at about the same pressure ratio. This pressure ratio is hereafter referred to as the optimum pressure ratio, and all further results are presented at the appropriate optimum pressure ratio for each case. Examination of figure 6 also shows that there is an optimum converter gas temperature ratio, and this optimum temperature ratio does not vary to any significant extent with changing pressure ratio. The optimum converter gas temperature ratio subsequently will be discussed further.

The effect of the ratio of cathode-to-anode temperature difference to converter inlet temperature, hereinafter called diode difference temperature ratio, on radiator area is presented in figure 7 for the primary and secondary radiators, as well as for the sum of the two radiators. As diode difference temperature ratio increases, primary radiator area, except at the very low end of the scale, increases and secondary radiator area decreases, thus resulting in a minimum for total radiator area. In the region of minimum total area for this case, the secondary radiator area is two to three times the primary radiator area.

Total radiator area is plotted against diode difference temperature ratio in figure 8 for several values of converter gas temperature ratio. Examination of figure 8 shows that for each value of diode difference temperature ratio there is one value of converter gas temperature ratio that results in a minimum area and that an envelope curve (dashed curve) drawn around the family of con-

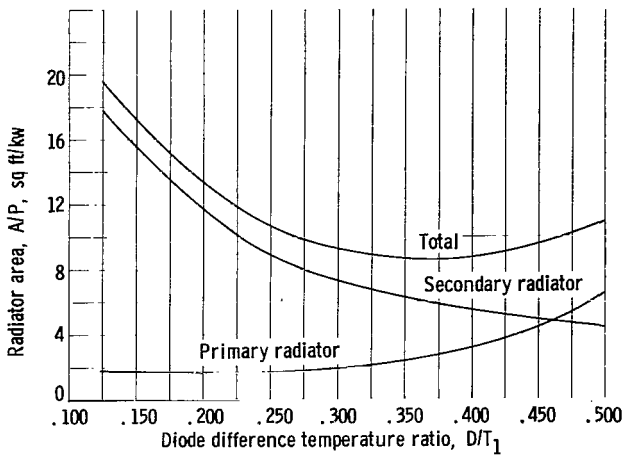


Figure 7. - Effect of diode difference temperature ratio on primary and secondary radiator areas for the Split Radiator cycle. Optimum compressor pressure ratio, 1.60; converter gas temperature ratio, 0.80.

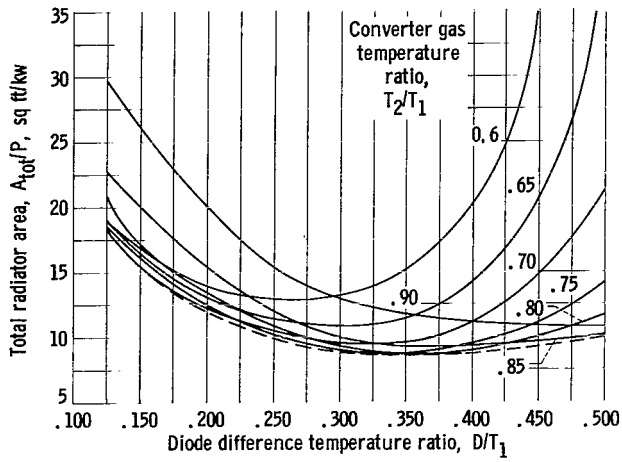


Figure 8. - Effect of diode difference and converter gas temperature ratios on total radiator area for Split Radiator cycle. Optimum compressor pressure ratio, 1.6.

verter gas temperature ratio curves shows a minimum area at some definite diode difference temperature ratio. Figures 5 to 8, consequently, show that all three variables can be optimized to yield a minimum radiator area.

The discussion and figures to follow will show how the design parameters affect both radiator area and the choice of cycle variables for the Split Radiator cycle. Envelope curves similar to the one shown in figure 8 are used to represent radiator area. The value of converter gas temperature ratio that minimizes radiator area at any given diode difference temperature ratio will be called the optimum converter gas temperature ratio and the loci of these are shown on the envelope curves. In addition, the optimum pressure ratios are also shown.

| Parameter | Parameter variation | | Radiator area reduction, percent |
|---|---|---|---|
| | From | To | |
| Converter inlet temperature, $T_1$ | 3000 | 3500 | 42 |
| | 3500 | 4000 | 38 |
| Ratio of actual to Carnot converter efficiency, $\psi$ | 0.3 | 0.6 | 53 |
| | .6 | 1.0 | 46 |
| Turbomachinery efficiency, $\eta_C$, $\eta_T$ | 0.7 | 0.8 | 47 |
| | .8 | .9 | 39 |
| Loss pressure ratio, $R_L$ | 0.7 | 0.8 | 35 |
| | .8 | .9 | 40 |
| Low-temperature-recuperator effectiveness, $E_{LT}$ | 0.0 | 0.5 | 10 |
| | .5 | 1.0 | 29 |
| High-temperature-recuperator effectiveness, $E_{HT}$ | 0.85 | 0.5 | 68 |
| | .5 | 0 | 24 |
| Secondary radiator heat-transfer coefficient, $h_R$ | 5 | 50 | 40 |
| | 50 | ∞ | 12 |

The effects of several of the more pertinent design parameters on minimum radiator area are presented in figures 9 to 15. These design parameters are seen to have very significant effects on the required radiator area. Some examples of these effects, as obtained from figures 9 to 15, are listed in the table at the left. Unless the achievable cycle parameters are known with some degree of certainty, the radiator requirements for this cycle cannot be established.

Over the wide range of

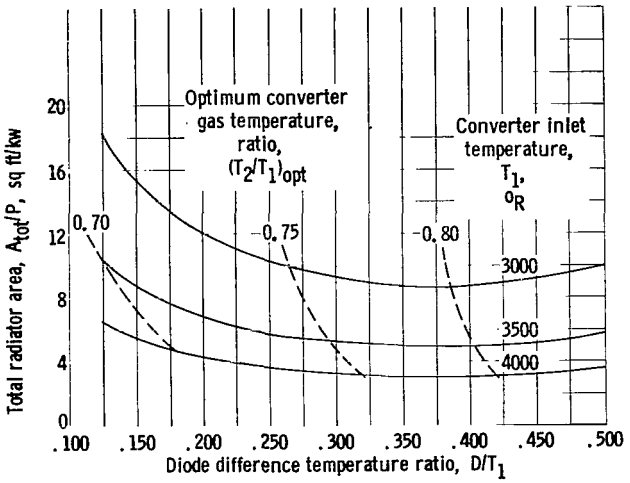


Figure 9. - Effect of converter inlet temperature on total radiator area for Split Radiator cycle. Optimum compressor pressure ratio, 1.6.

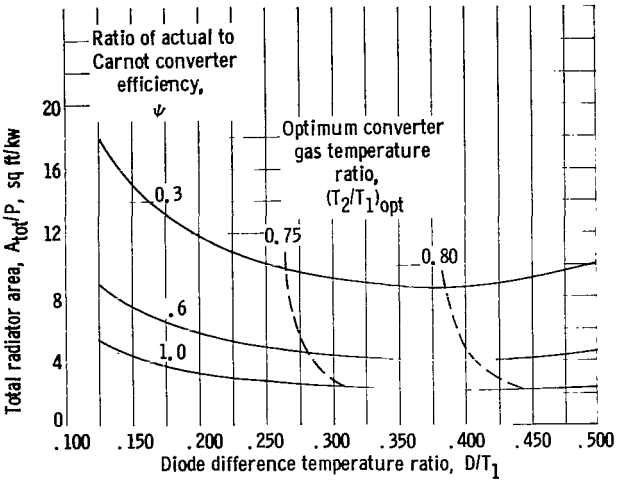


Figure 10. - Effect of converter efficiency on total radiator area for Split Radiator cycle. Optimum compressor pressure ratio, 1.6.

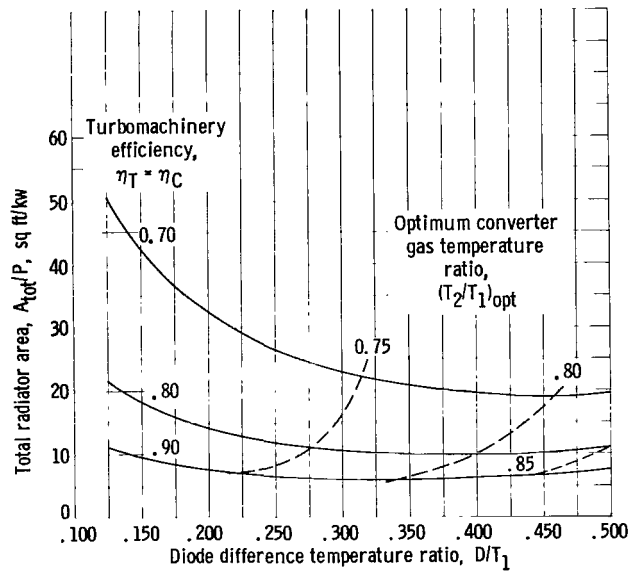


Figure 11. - Effect of turbomachinery efficiency on total radiator area for Split Radiator cycle. Optimum compressor pressure ratio, 1.6.

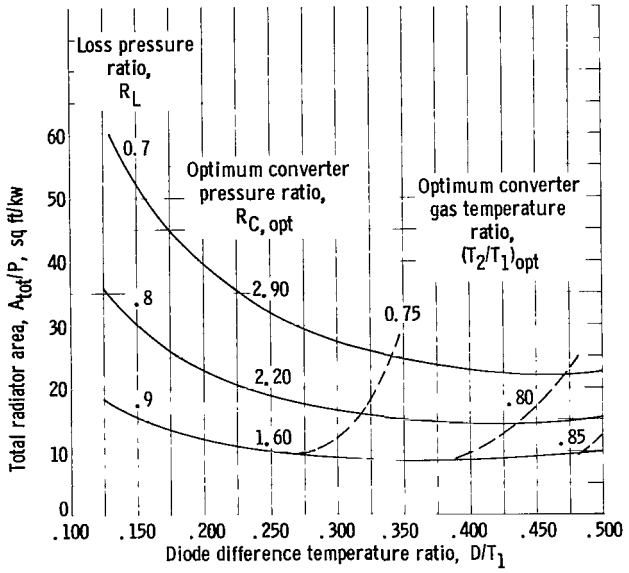


Figure 12. - Effect of loss pressure ratio on total radiator area for Split Radiator cycle.

design parameter values considered in this study, the optimum values for compressor pressure ratio, diode difference temperature ratio, and converter gas temperature ratio at the minimum point were generally in the range of 1.45 to 2.20, 0.35 to 0.45, and 0.78 to 0.82, respectively.

## Thermionic Gas Cycle Comparison

The Two Loop and Turbineless cycles were optimized in a manner similar to

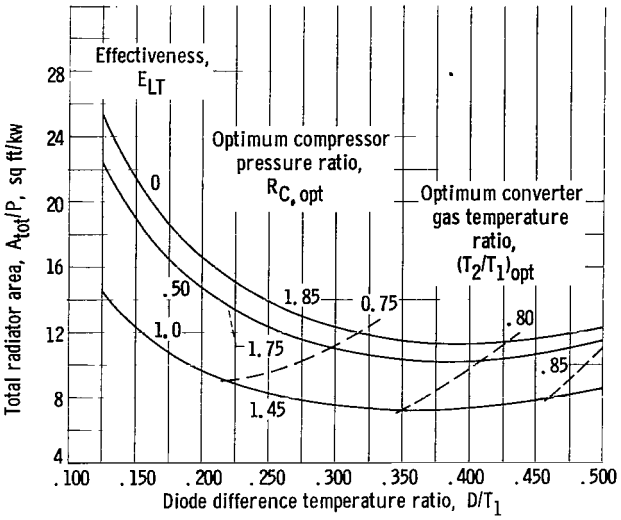


Figure 13. - Effect of low-temperature-recuperator effectiveness on total radiator area for Split Radiator cycle.

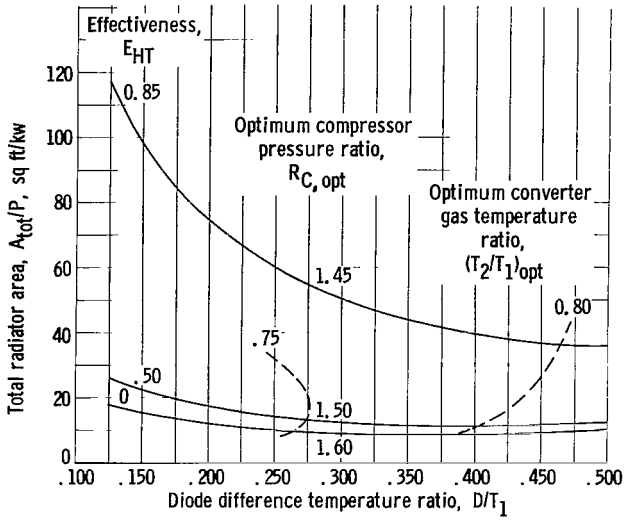


Figure 14. - Effect of high-temperature-recuperator effectiveness on total radiator area for Split Radiator cycle.

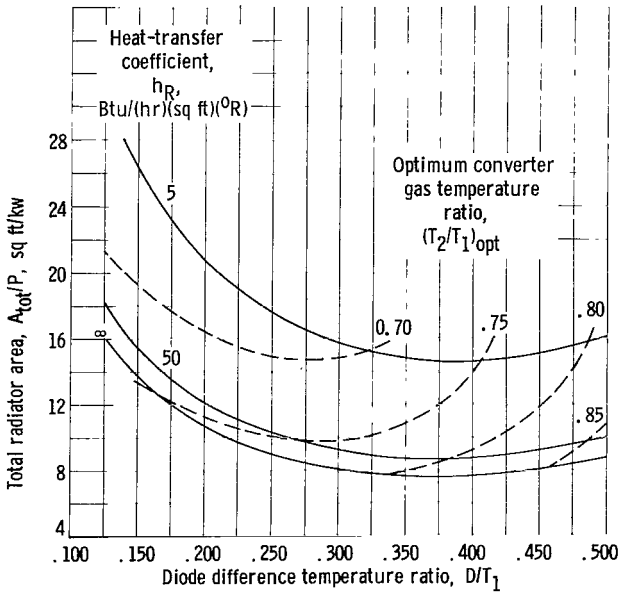


Figure 15. - Effect of gas heat-transfer coefficient on total radiator area for Split Radiator cycle. Optimum compressor pressure ratio, 1.6.

that just shown for the Split Radiator cycle, and it is the purpose of this section to compare the minimum radiator areas for the three cycles. These radiator areas were computed using the previously tabulated cycle parameters. The radiator area comparison is made on the basis of maximum cycle temperature and, for those cycles having turbines, also on the basis of turbine inlet temperature since either one of these temperatures may be the limiting condition. Minimum radiator area is plotted against maximum cycle temperature in figure 16(a) for all three cycles. It can be seen that for any given maximum

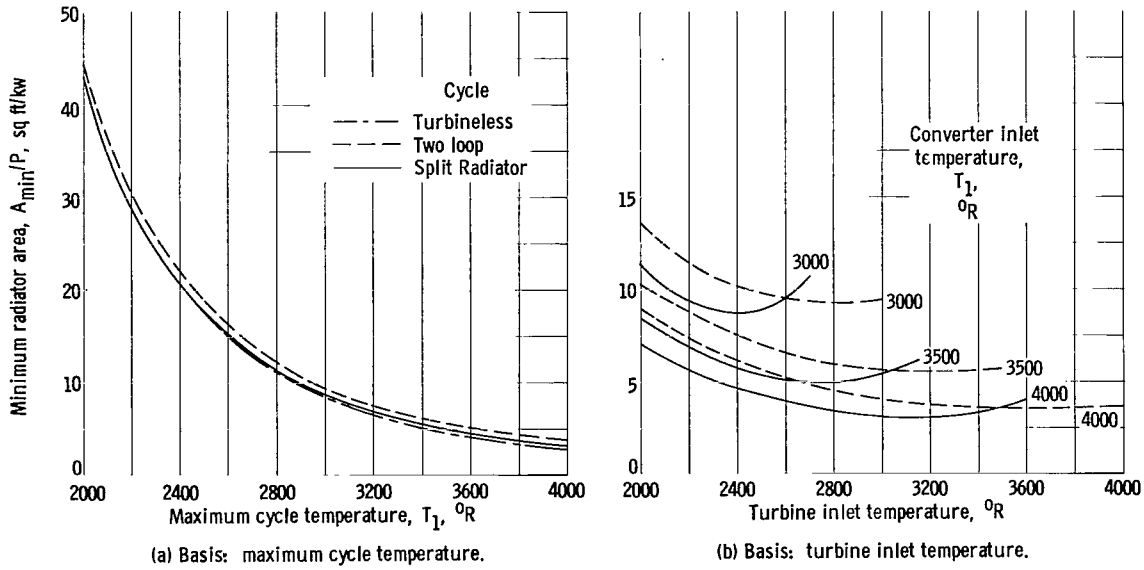


Figure 16. - Radiator area comparison for thermionic gas cycles.

cycle temperature, the radiator area requirements for the three cycles are comparable. It must be emphasized that the results of this and all subsequent comparisons depend upon the design parameter values used. Although the selected parameter values are believed to be reasonable, there exists sufficient latitude of choice such that the results of any radiator area comparison can be significantly affected. All comparisons, therefore, must be viewed in the light of the assumed parameter values.

Minimum radiator area is plotted against turbine inlet temperature in figure 16(b) for several values of maximum cycle temperature for the Split Radiator and Two Loop cycles. Although the radiator area requirements for these two cycles are comparable on the basis of maximum cycle temperature, it is seen from figure 16(b) that the minimum area for the Split Radiator cycle is achieved with a turbine inlet temperature several hundred degrees lower than that required for the Two Loop cycle. The radiator area curves, however, are relatively flat with respect to turbine inlet temperature, and for any given turbine inlet temperature, the Two Loop cycle does not require significantly more radiator area than does the Split Radiator cycle. On the basis of these radiator area comparisons, none of the three out-of-pile thermionic gas cycles appears to be markedly superior to the other two.

## Comparison with Brayton Cycle

The radiator area requirements for an optimized Split Radiator cycle will now be compared to those for an optimized Brayton cycle in order to determine whether an out-of-pile thermionic gas cycle possesses any radiator area advantages over a turboelectric gas cycle. Schematic and temperature-entropy diagrams for the Brayton cycle are presented in figure 17. This comparison is

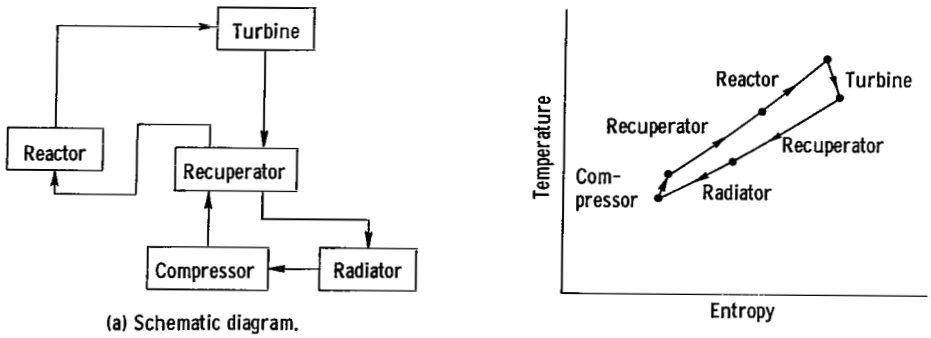


(a) Schematic diagram.

(b) Temperature-entropy diagram.

Figure 17. - Brayton cycle.

made first on the basis of the previously discussed ideal analysis and then incorporates the nonideal considerations for the Split Radiator cycle. Except where otherwise indicated, the design parameters used for the optimized cycles are those that were previously tabulated. The design parameters and radiator areas for the optimized Brayton cycle were obtained from reference 6, where radiator area was computed on a basis similar to that used in this analysis. The radiator areas from reference 6 were adjusted to the basis of electrical power output by assuming a generator efficiency of 0.90 for use in this comparison.

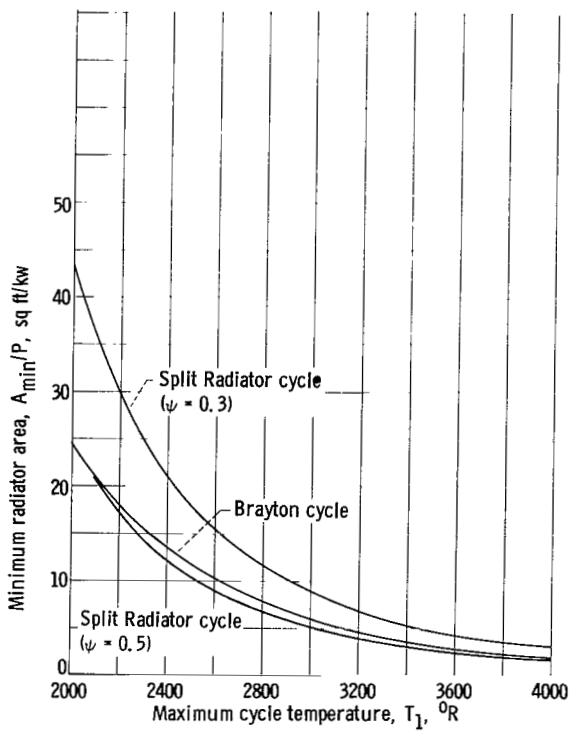


Figure 18. - Minimum radiator area comparison of Split Radiator cycle with Brayton cycle (basis: maximum cycle temperature, ideal analysis).

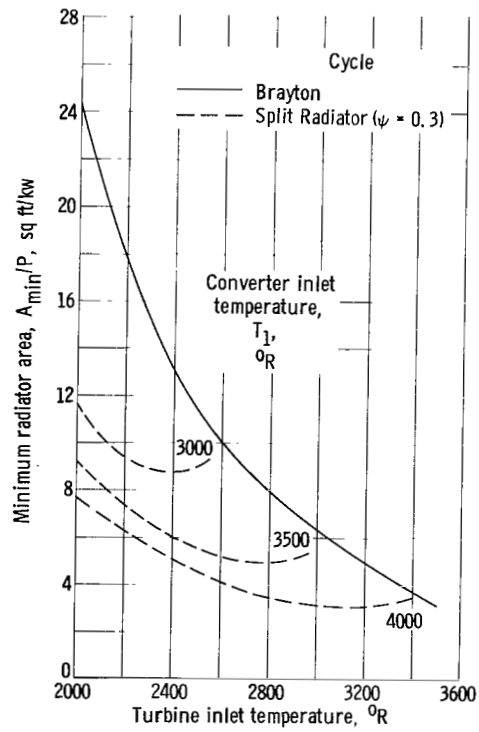


Figure 19. - Minimum radiator area comparison of Split Radiator cycle with Brayton cycle (basis: turbine inlet temperature, ideal analysis).

Minimum radiator area is plotted against maximum cycle temperature in figure 18 for the Split Radiator cycle and the Brayton cycle. Both figures 18 and 19 are based on the ideal analysis for the Split Radiator cycle. On the basis of equal maximum cycle temperature, a Split Radiator cycle with a 0.3 ratio of actual to Carnot converter efficiency requires about 50 percent more radiator area than a Brayton cycle. In order for the two cycles to exhibit comparable radiator area requirements, the Split Radiator cycle must achieve about a 0.5 ratio of actual to Carnot converter efficiency.

Minimum radiator area is plotted against turbine inlet temperature in figure 19 for the Brayton cycle and for the Split Radiator cycle with converter inlet temperatures of 3000° , 3500° , and 4000° R. On the basis of equal turbine inlet temperature, the Split Radiator cycle with a 0.3 ratio of actual to Carnot converter efficiency is seen to offer a significant radiator area reduction when compared to the Brayton cycle. For example, at a turbine inlet temperature of 2400° R, the indicated radiator area reductions are 33, 55, and 61 percent for converter inlet temperatures of 3000° , 3500° , and 4000° R, respectively. A reduction in achievable converter efficiency rapidly dissipates the potential savings.

Figure 20 presents the radiator area comparisons that were made on the basis of the experimentally determined converter efficiencies reported in references 4 and 5 and shown in figure 4. In addition, the effect of gas-to-cathode temperature differences is explored parametrically by assuming gas-to-cathode temperature ratios of 1.0, 1.05, and 1.1 in figures 20(a), (b), and (c), respectively. Minimum radiator area is plotted against turbine inlet temperature in these figures for the Split Radiator cycle with several converter inlet temperatures and for the Brayton cycle. On the basis of equal maximum cycle temperatures (converter inlet for the Split Radiator cycle and turbine inlet for the Brayton cycle), the Split Radiator cycle requires significantly more radiator area than the Brayton cycle. On the basis of equal turbine inlet temperature, it can be seen from figure 20(a) that, even with ideal heat transfer between gas and cathode, converter inlet temperatures of about 3500° R and higher are required if the Split Radiator cycle is to have any significant radiator area advantage over the Brayton cycle. As the gas-to-cathode temperature ratio increases (figs. 20(b) and (c)), the radiator area required for the Split Radiator cycle increases due to a decrease in cathode temperature and, consequently, in converter efficiency. With a gas-to-cathode temperature ratio of 1.1, as shown in figure 20(c), a converter inlet temperature of at least about 4000° R is required if the Split Radiator cycle is to have any radiator area advantage over a Brayton cycle. With the experimental converter efficiencies used in this analysis, extremely high converter inlet temperatures of at least 3500° to 4000° R and, consequently, even higher reactor operating temperatures are required if the Split Radiator cycle is to be competitive with a turboelectric Brayton cycle on the basis of radiator area. As thermionic converters improve and achievable efficiencies increase, the potential of the Split Radiator cycle will increase accordingly.

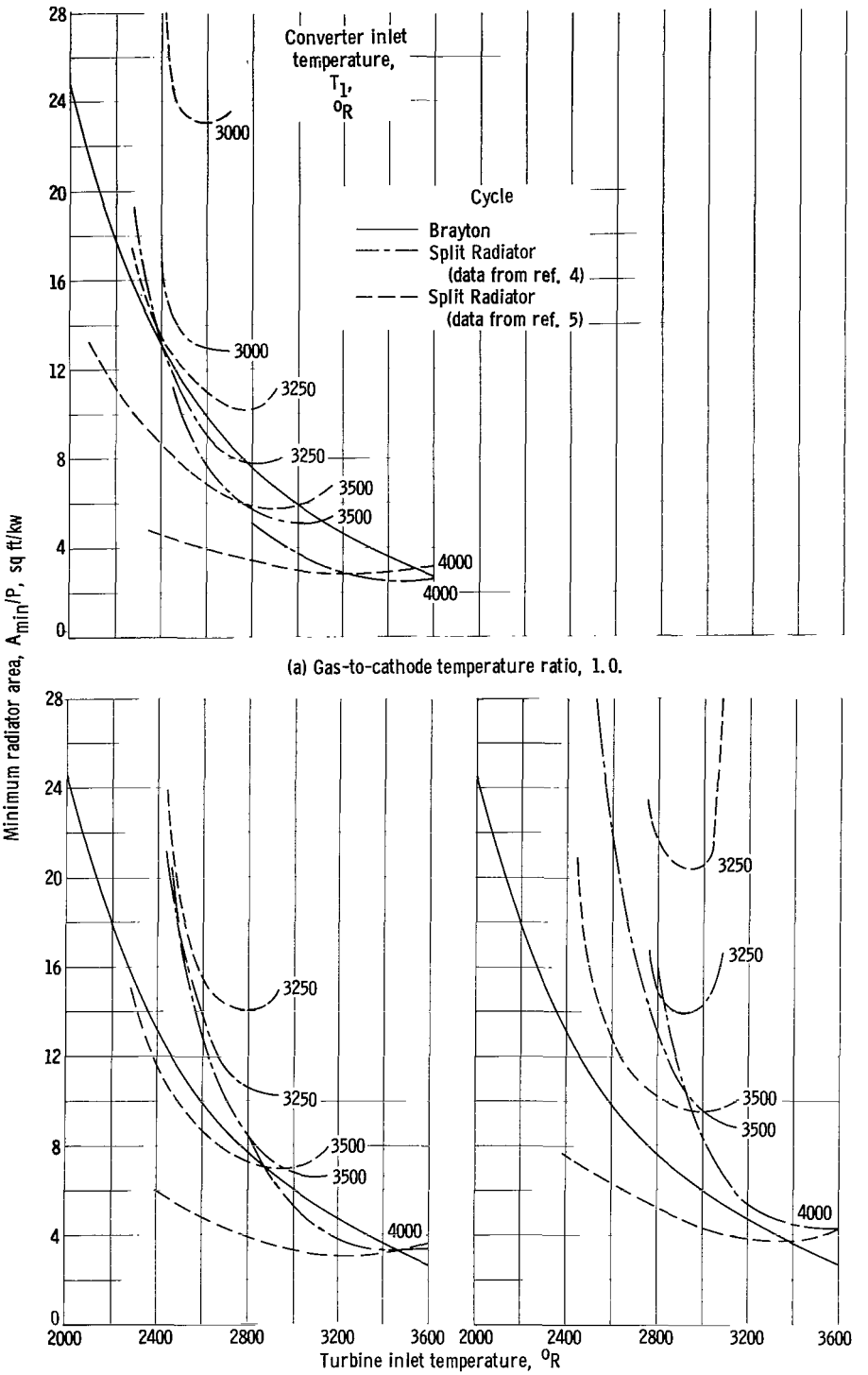


(a) Gas-to-cathode temperature ratio, 1.0.

(b) Gas-to-cathode temperature ratio, 1.05.

(c) Gas-to-cathode temperature ratio, 1.1.

Figure 20. - Minimum radiator area comparison of Split Radiator cycle with Brayton cycle (basis: turbine inlet temp., experimental converter efficiencies).

## SUMMARY OF RESULTS

The radiator area potential of out-of-pile thermionic space power systems using an inert gas as the heat-transfer medium was assessed by studying the radiator area characteristics of three typical out-of-pile systems and comparing minimum radiator area requirements with those for a turboelectric Brayton cycle. Three cycles were chosen for preliminary investigation: the Split Radiator cycle, the Two Loop cycle, and the Turbineless cycle. This analysis was primarily a thermodynamic cycle analysis, and the only imposed converter limitation was with respect to efficiency, which was treated both parametrically and through the use of experimental data. The pertinent results of this analysis are summarized as follows:

1. The minimum radiator areas for the three out-of-pile thermionic gas cycles were compared on the basis of equal maximum cycle temperature and, for those cycles having turbines, also on the basis of equal turbine inlet temperature. No significant differences in radiator area requirements were found among the three cycles.

2. The radiator area required for the Split Radiator cycle was compared with that for the Brayton cycle on the basis of a parametric variation in converter efficiency and ideal gas-to-cathode heat transfer in the converter. With the two cycles operating at the same maximum temperature, the Split Radiator cycle must be able to achieve about a 0.5 ratio of actual to Carnot converter efficiency in order to require the same radiator area as the Brayton cycle. On the basis of equal turbine inlet temperatures, a Split Radiator cycle with a 0.3 ratio of actual to Carnot converter efficiency offers a significant reduction in radiator area when compared with a Brayton cycle.

3. The radiator area required for the Split Radiator cycle was also compared with that for a Brayton cycle on the basis of experimentally determined converter efficiencies and a parametric variation in the gas-to-cathode temperature difference. With the two cycles operating at the same maximum temperature, the Split Radiator cycle requires more radiator area than the Brayton cycle. On the basis of equal turbine inlet temperatures, converter inlet temperatures greater than $3500^{\circ}$ R are required for the Split Radiator cycle if it is to have any radiator area advantage over the Brayton cycle.

## CONCLUDING REMARKS

Radiator area was shown to be extremely sensitive to variations in the cycle design parameters (converter inlet temperature, converter efficiency, turbomachinery efficiency, loss pressure ratio, and recuperator effectiveness). Although the selected design parameters were believed to be reasonable, there exists sufficient latitude of choice such that the results of any radiator area comparison can be significantly affected. In addition, the pertinent parameters and their significances differ to some extent for the different cycles studied and compared. All comparisons, therefore, must be viewed in the

light of the assumed parameter values for each of the cycles being compared.

Lewis Research Center
National Aeronautics and Space Administration
Cleveland, Ohio, May 13, 1964

## APPENDIX A

### DERIVATION OF EFFICIENCY, CAPACITY RATE, AND TEMPERATURE EQUATIONS FOR THE SPLIT RADIATOR CYCLE

Thermionic converter efficiency, in this study, is expressed as the product of the ideal efficiency (Carnot) and a parameter ($\psi$) representing the ratio of actual to ideal efficiency

$$\eta_{th} = \psi \eta_{th,i} \tag{A1}$$

Since the anode and cathode temperatures vary along the length of the converter, an average ideal efficiency must be obtained. Ideal converter output can be expressed as

$$3415.0\ P_i = \eta_{th,i,av} Q_s = \int_{inlet}^{exit} \eta_{th,i}\ dQ_s \tag{A2a}$$

and, consequently,

$$\eta_{th,i,av} = \frac{1}{Q_s} \int_{inlet}^{exit} \eta_{th,i}\ dQ_s \tag{A2b}$$

Since any differential element of the converter can be considered as a heat engine with constant temperature heat addition and rejection, the local ideal efficiency is merely the Carnot efficiency,

$$\eta_{th,i} = \frac{T_c - T_a}{T_c} = \frac{D}{T_c} \tag{A3}$$

where, in order to simplify the analysis, D is assumed constant throughout the converter. The total and differential amounts of heat supplied to the cathode are

$$Q_s = wc_p(T_1 - T_2) \tag{A4a}$$

and

$$dQ_s = -wc_p\ dT_g \tag{A4b}$$

Substituting equations (A3) to (A4b) into equation (A2b), setting $dT_g = dT_c$, and integrating from $T_c = T_1$ to $T_c = T_2$ yield

$$\eta_{th,i,av} = \frac{D}{T_1 - T_2} \ln \frac{T_1}{T_2} \tag{A5a}$$

or, on a temperature ratio basis,

$$\eta_{th,i,av} = \frac{D/T_1}{1 - (T_2/T_1)} \ln \frac{T_1}{T_2} \tag{A5b}$$

Fluid specific capacity rate, $wc_p/P$, is obtained by considering the actual output from the converter, that is

$$3415.0\ P = \eta_{th} Q_s = \psi \eta_{th,i,av} wc_p (T_1 - T_2) \tag{A6}$$

Substitution of equation (A5b) into equation (A6) and rearrangement result in

$$\frac{wc_p}{P} = \frac{3415.0}{\psi T_1 (D/T_1) \ln(T_1/T_2)} \tag{A7}$$

Cycle efficiency is equal to converter output divided by the heat added to the system, that is,

$$\eta_{cy} = \frac{\psi \eta_{th,i,av} wc_p (T_1 - T_2)}{wc_p (T_1 - T_9)} \tag{A8a}$$

Cancelling $wc_p$ and dividing by $T_1$ give

$$\eta_{cy} = \frac{\psi \eta_{th,i,av} (1 - T_2/T_1)}{1 - T_9/T_1} \tag{A8b}$$

The reactor inlet to converter inlet temperature ratio, $T_9/T_1$, can be expressed as a function of the cycle parameters (turbomachinery efficiencies, recuperator effectiveness, and loss pressure ratio) and two cycle variables. The cycle variables selected for the expression of $T_9/T_1$ are $T_2/T_1$, which has already appeared in several equations, and compressor pressure ratio, $R_C$. For purposes of brevity in the following development, $T_{jk}$ and $p_{jk}$ are used to represent $T_j/T_k$ and $p_j/p_k$, respectively. By using this convention, equation (A8b) becomes

$$\eta_{cy} = \frac{\psi \eta_{th,i,av} (1 - T_{21})}{1 - T_{91}} \tag{A8c}$$

Development of the expression for $T_{91}$, as well as expressions for the ratios of other system temperatures to $T_1$, is given in the same sequence as would be used for computation in order to facilitate comprehension. Compressor work can be expressed as

$$\Delta h_C = wc_p (T_7 - T_6) = wc_p \frac{(T_{7i} - T_6)}{\eta_C} \tag{A9a}$$

Dividing both sides by $wc_p T_6$ and using the isentropic state equation

$$T_{7i6} = p_{76}^{\frac{\gamma-1}{\gamma}}$$

result in

$$T_{76} - 1 = \frac{1}{\eta_C}\left(p_{76}^{\frac{\gamma-1}{\gamma}} - 1\right) \tag{A9b}$$

Setting $p_{76} = R_C$ and rearranging equation (A9b) yield

$$T_{76} = 1 + \frac{1}{\eta_C}\left(R_C^{\frac{\gamma-1}{\gamma}} - 1\right) \tag{A9c}$$

A similar consideration for the turbine shows that

$$T_{43} = 1 - \eta_T\left(1 - \frac{1}{R_T^{\frac{\gamma-1}{\gamma}}}\right) \tag{A10}$$

where, by definition, $R_T = p_{34}$. The compressor and turbine pressure ratios are related by the loss pressure ratio, which is equal to the product of the ratio of exit to inlet pressure in all the heat-transfer components. This relation is

$$p_{34} = (p_{87}p_{98}p_{19}p_{21}p_{32}p_{54}p_{65})p_{76} \tag{A11a}$$

or

$$R_T = R_L R_C \tag{A11b}$$

Substitution of equation (A11b) into equation (A10) yields the following expression:

$$T_{43} = 1 - \eta_T\left[1 - (R_L R_C)^{\frac{1-\gamma}{\gamma}}\right] \tag{A12}$$

Turbine work equals compressor work, which can be expressed as

$$T_4 - T_3 = T_6 - T_7 \tag{A13a}$$

Dividing equation (A13a) by $T_6$, recognizing that $T_{46} = T_{43}T_{36}$, and solving for $T_{36}$ give

$$T_{36} = \frac{T_{76} - 1}{1 - T_{43}} \tag{A13b}$$

and $T_{46}$ is obtained as

$$T_{46} = T_{43}T_{36} \tag{A14}$$

The remaining temperature ratios are obtained by considering the two recuperators. The effectiveness of the low temperature recuperator can be expressed as

$$E_{LT} = \frac{T_4 - T_5}{T_4 - T_7} \tag{A15a}$$

Solving equation (A15a) for $T_5$ and dividing by $T_6$ yield

$$T_{56} = T_{46} - E_{LT}(T_{46} - T_{76}) \tag{A15b}$$

A heat balance, with all values divided by $T_6$, around the low temperature recuperator results in

$$T_{86} = T_{46} - T_{56} + T_{76} \tag{A16}$$

The effectiveness of the high temperature recuperator is

$$E_{HT} = \frac{T_2 - T_3}{T_2 - T_8} \tag{A17a}$$

Dividing by $T_6$ and solving for $T_{26}$ give

$$T_{26} = \frac{T_{36} - E_{HT}T_{86}}{1 - E_{HT}} \tag{A17b}$$

and a heat balance around the high temperature recuperator results in

$$T_{96} = T_{26} - T_{36} + T_{86} \tag{A18}$$

All temperatures have now been related to $T_6$; it is, however, desired to relate them to $T_1$. This is accomplished by using the previously specified cycle temperature variable $T_{21}$ as follows:

$$T_{61} = \frac{T_{21}}{T_{26}} \tag{A19}$$

$$T_{j1} = T_{j6}T_{61} \qquad j = 3, 4, \ldots, 9 \tag{A20}$$

Specification of any set of cycle parameters ($\eta_T$, $\eta_C$, $\Psi$, $R_L$, $E_{LT}$, $E_{HT}$, and $T_1$) and variables ($T_2/T_1$, $D/T_1$, and $R_C$), therefore, allows the computation of converter efficiency, (eqs. (A5) and (1)), cycle efficiency

(eq. (A8c)), fluid specific capacity rate (eq. (A7)), and all temperatures around the cycle (eqs. (A9) to (A20)).

## APPENDIX B

## DERIVATION OF EFFICIENCY, CAPACITY RATE, AND TEMPERATURE EQUATIONS FOR THE TWO LOOP CYCLE

For this cycle, as for the Split Radiator cycle, equations (A1) to (A4b) apply. Substituting equations (A3) to (A4b) into equation (A2b) and setting $dT_g = dT_c$ yield

$$\eta_{th,i,av} = \frac{1}{T_1 - T_2} \int_{T_2}^{T_1} \frac{D}{T_c}\, dT_c \tag{B1}$$

Since D is nct constant for this case, equation (B1) cannot be integrated until D can be expressed in terms of $T_c$. For a differential element of converter, the heat supplied by the hot loop (loop I) gas is only partially converted to electricity with the remainder being added to the cold loop (loop II) gas. Therefore,

$$w_{II} c_p\, dT_a = (1 - \eta_{th}) w_I c_p\, dT_c \tag{B2}$$

Substituting equations (A1) and (A3) into equation (B2) and letting

$$dT_a = dT_c - dD$$

result in

$$w_{II}\, dT_c - w_{II}\, dD = \left(1 - \psi \frac{D}{T_c}\right) w_I\, dT_c \tag{B3a}$$

Rearranging equation (B3a) gives

$$\frac{dD}{dT_c} = 1 - \frac{w_I}{w_{II}} + \frac{w_I}{w_{II}} \psi \frac{D}{T_c} \tag{B3b}$$

This is a first-order differential equation that can be solved by any standard textbook method. Using the boundary condition $D = D_1$ when $T_c = T_1$ results in the solution

$$\frac{D}{T_c} = \frac{1 - \frac{w_I}{w_{II}} - \left[1 - \frac{w_I}{w_{II}} - \frac{D_1}{T_1}\left(1 - \psi \frac{w_I}{w_{II}}\right)\right]\left(\frac{T_1}{T_c}\right)^{1 - \psi \frac{w_I}{w_{II}}}}{1 - \psi \frac{w_I}{w_{II}}} \tag{B4}$$

Substituting equation (B4) into equation (B1), performing the indicated integration, and dividing by $T_1$ yield

$$\eta_{th,i,av} = \frac{1 - \frac{w_I}{w_{II}}}{1 - \psi \frac{w_I}{w_{II}}} - \frac{\left[1 - \frac{w_I}{w_{II}} - \frac{D_1}{T_1}\left(1 - \psi \frac{w_I}{w_{II}}\right)\right]\left[1 - \left(\frac{T_2}{T_1}\right)^{\psi \frac{w_I}{w_{II}}}\right]}{\left(1 - \psi \frac{w_I}{w_{II}}\right)\left(\psi \frac{w_I}{w_{II}}\right)\left(1 - \frac{T_2}{T_1}\right)} \tag{B5}$$

Fluid specific capacity rate must be obtained for both loops in this cycle. For the hot loop, equation (A6) applies, except that for this case $w = w_I$. Consequently, rearrangement of equation (A6) gives

$$\frac{w_I c_p}{P} = \frac{3415.0}{\psi \eta_{th,i,av} T_1 \left(1 - \frac{T_2}{T_1}\right)} \tag{B6}$$

The fluid specific capacity rate for the cold loop can be expressed as

$$\frac{w_{II} c_p}{P} = \frac{\frac{w_I c_p}{P}}{\frac{w_I}{w_{II}}} \tag{B7}$$

The ratio $w_I/w_{II}$, which appears in both equations (B5) and (B7), is not an independent variable but can be calculated as will be shown later.

Cycle efficiency can be expressed as

$$\eta_{cy} = \frac{\psi \eta_{th,i,av}(1 - T_2/T_1)}{1 - T_9/T_1} \tag{B8}$$

which is the same as equation (A8b) except that $\eta_{th,i,av}$ is here evaluated from equation (B5). As in appendix A, $T_9/T_1$ will be expressed in terms of the cycle parameters and variables. For this cycle, the selected variables are $T_2/T_1$, $D_1/T_1$, and $R_{C,II}$. The previously used convention for expressing temperature and pressure ratios is here again used.

Compressor work for loop I can be expressed as

$$\Delta h_{C,I} = w_I c_p (T_9 - T_2) = w_I c_p \frac{(T_{9i} - T_2)}{\eta_{C,I}} \tag{B9a}$$

Dividing both sides by $w_I c_p T_2$ and using the isentropic state equation

$$T_{9i2} = p_{92}^{\frac{\gamma-1}{\gamma}}$$

yield

$$T_{92} = 1 + \frac{1}{\eta_{C,I}}\left(p_{92}^{\frac{\gamma-1}{\gamma}} - 1\right) \tag{B9b}$$

The loss pressure ratio for loop I is equal to the reciprocal of the compressor pressure ratio, that is,

$$R_{L,I} = p_{19}p_{21} = p_{29} = \frac{1}{p_{92}} \tag{B10}$$

Substituting equation (B10) into equation (B9b) and setting

$$T_{92} = \frac{T_{91}}{T_{21}}$$

result in

$$T_{91} = T_{21}\left[1 + \frac{1}{\eta_{C,I}}\left(R_{L,I}^{\frac{1-\gamma}{\gamma}} - 1\right)\right] \tag{B11}$$

For loop II, certain of the compressor and turbine considerations are similar to those for the Split Radiator cycle, so that, with a minor change in nomenclature, equations (A9a) to (A12) can be applied with the exception that

$$R_{L,II} = p_{87}p_{38}p_{54}p_{65} \tag{B12}$$

The pertinent relations, equations (A9c) and (A12), as would be applied to loop II of this cycle, are

$$T_{76} = 1 + \frac{1}{\eta_{C,II}}\left(R_{C,II}^{\frac{\gamma-1}{\gamma}} - 1\right) \tag{B13}$$

and

$$T_{43} = 1 - \eta_T\left[1 - \left(R_{L,II}R_{C,II}\right)^{\frac{1-\gamma}{\gamma}}\right] \tag{B14}$$

The ratios of turbine inlet and exit temperatures to $T_1$ are evaluated as follows:

$$T_{31} = 1 - \frac{D_1}{T_1} \tag{B15}$$

$$T_{41} = T_{43}T_{31} \tag{B16}$$

The work done by the turbine must equal the work required for the two compressors, therefore,

$$w_I(T_9 - T_2) + w_{II}(T_7 - T_6) = w_{II}(T_3 - T_4) \tag{B17a}$$

Dividing equation (B17a) by $T_1$, recognizing that $T_{71} = T_{76}T_{61}$, and solving for $T_{61}$ yield

$$T_{61} = \frac{T_{31} - T_{41} - \frac{w_I}{w_{II}}(T_{91} - T_{21})}{T_{76} - 1} \tag{B17b}$$

If $w_I/w_{II}$ were known, $T_{61}$ could be evaluated and $T_{71}$ obtained from

$$T_{71} = T_{76}T_{61} \tag{B18}$$

Consideration of the heat exchangers leads to the evaluation of $w_I/w_{II}$ as well as the remaining temperature ratios. The effectiveness of the recuperator can be expressed as

$$E = \frac{T_8 - T_7}{T_4 - T_7} \tag{B19a}$$

Dividing by $T_1$ and solving for $T_{81}$ result in

$$T_{81} = ET_{41} + (1 - E)T_{71} \tag{B19b}$$

Substitution of equations (B17b) and (B18) into equation (B19b) gives

$$T_{81} = ET_{41} + (1 - E)T_{76}\left[\frac{T_{31} - T_{41} - \frac{w_I}{w_{II}}(T_{91} - T_{21})}{T_{76} - 1}\right] \tag{B20}$$

Another equation for $T_{81}$ in terms of $w_I/w_{II}$ can be obtained by evaluating equation (B4) at the cold end of the heat exchanger where $D = T_2 - T_8$ and $T_c = T_2$. Making this substitution and solving equation (B4) for $T_{81}$ yield

$$T_{81} = T_{21}\left\{1 - \frac{1 - \frac{w_I}{w_{II}} - \left[1 - \frac{w_I}{w_{II}} - \frac{D_1}{T_1}\left(1 - \psi\frac{w_I}{w_{II}}\right)\right](T_{21})^{\psi\frac{w_I}{w_{II}} - 1}}{1 - \psi\frac{w_I}{w_{II}}}\right\} \tag{B21}$$

Simultaneous solution of equations (B20) and (B21) gives unique values for $T_{81}$ and $w_I/w_{II}$. With $w_I/w_{II}$ known, $T_{61}$ and $T_{71}$ are evaluated from equations (B17b) and (B18), respectively. A heat balance around the recuperator yields $T_{51}$

$$T_{51} = T_{71} - T_{81} + T_{41} \tag{B22}$$

Specification of any set of cycle parameters ($\eta_T$, $\eta_{C,I}$, $\eta_{C,II}$, $\Psi$, $R_{L,I}$, $R_{L,II}$, E, and $T_1$) and variables ($T_2/T_1$, $D_1/T_1$, and $R_{C,II}$), therefore, allows the computation of converter efficiency (eqs. (B5) and (A1)), cycle efficiency (eq. (B8)), fluid specific capacity rate for both loops (eqs. (B6) and (B7)), and all temperatures around the cycle (eqs. (B9) to (B22)).

## APPENDIX C

## DERIVATION OF EFFICIENCY, CAPACITY RATE, AND TEMPERATURE EQUATIONS FOR THE TURBINELESS CYCLE

The converter efficiency characteristics for this cycle are similar to those for the Split Radiator cycle, and equations (A1) to (A5b) also apply to this cycle. As stated by equation (A5b),

$$\eta_{th,i,av} = \frac{D/T_1}{1 - (T_2/T_1)} \ln \frac{T_1}{T_2} \tag{C1}$$

Fluid specific capacity rate is obtained by considering the net output from the converter since a portion of the total output is recycled to the compressor motor. Therefore,

$$3415.0\ P_n = \psi\eta_{th,i,av} wc_p(T_1 - T_2) - wc_p(T_3 - T_2)/\eta_m \tag{C2}$$

Substitution of equation (C1) into equation (C2) and rearrangement yield

$$\frac{wc_p}{P_n} = \frac{3415.0}{\psi T_1(D/T_1) \ln (T_1/T_2) - T_1(T_3/T_1 - T_2/T_1)/\eta_m} \tag{C3}$$

Cycle efficiency is equal to the converter net output divided by system heat input or

$$\eta_{cy} = \frac{\psi\eta_{th,i,av} wc_p(T_1 - T_2) - wc_p(T_3 - T_2)/\eta_m}{wc_p(T_1 - T_3)} \tag{C4a}$$

Cancelling $wc_p$ and dividing by $T_1$ result in

$$\eta_{cy} = \frac{\psi\eta_{th,i,av}(1 - T_2/T_1) - (T_3/T_1 - T_2/T_1)/\eta_m}{1 - T_3/T_1} \tag{C4b}$$

For this cycle, only $T_3/T_1$ remains to be evaluated.

Compressor work can be expressed as

$$\Delta h_C = wc_p(T_3 - T_2) = wc_p \frac{(T_{3i} - T_2)}{\eta_C} \tag{C5a}$$

Dividing both sides of equation (C5a) by $wc_pT_2$ and using the isentropic state equation

$$T_{3i2} = p_{32}^{\frac{\gamma-1}{\gamma}}$$

give

$$T_{32} = 1 + \frac{1}{\eta_C}\left(p_{32}^{\frac{\gamma-1}{\gamma}} - 1\right) \tag{C5b}$$

The loss pressure ratio is equal to the reciprocal of the compressor pressure ratio

$$R_L = p_{21}p_{13} = p_{23} = \frac{1}{p_{32}} \tag{C6}$$

Substituting equation (C6) into equation (C5b) and letting $T_{32} = T_{31}/T_{21}$ yield

$$T_{31} = T_{21}\left[1 + \frac{1}{\eta_C}\left(R_L^{\frac{1-\gamma}{\gamma}} - 1\right)\right] \tag{C7}$$

Specification of any set of cycle parameters ($\eta_C$, $\eta_m$, $\psi$, $R_L$, and $T_1$) and variables ($T_2/T_1$ and $D/T_1$) now allows the computation of converter efficiency (eqs. (C1) and (A1)), cycle efficiency (eq. (C4b)), fluid specific capacity rate (eq. (C3)), and all temperatures around the cycle (eq. (C7)).

## REFERENCES


1. Evvard, John C.: Non-Chemical Propulsion. Paper presented at Sixth Annual Missile and Space Tech. Inst., Univ. Connecticut, Aug. 9, 1963.

2. Grey, Jerry, and Williams, Peter M.: Re-Examination of Gas-Cycle Nuclear-Electric Space Powerplants. AIAA Jour., vol. 1, no. 12, Dec. 1963, pp. 2801-2811.

3. Bernatowicz, Daniel T.: A Parametric Study of the Thermionic Diode System for Large Nuclear-Electric Powerplants in Space Vehicles. NASA TN D-1110, 1962.

4. Grey, Jerry, and Williams, Peter M.: Analyses of Gas-Cycle and Hybrid Nuclear-Space Power Systems. Paper presented at Int. Astronautical Cong., Paris (France), Sept. 26-Oct. 1, 1963.

5. Kitrilakis, S. S., Meeker, M. E., and Rasor, N. S.: Annual Technical Summary Report for the Thermionic Emitter Materials Research Program. TEE 4015-3, Thermo Electron Eng. Corp., July 1, 1961-June 30, 1962.

6. Glassman, Arthur J., and Stewart, Warner L.: A Look at the Thermodynamic Characteristics of Brayton Cycles for Space Power. Paper 63-218, AIAA, 1963.

*"The aeronautical and space activities of the United States shall be conducted so as to contribute . . . to the expansion of human knowledge of phenomena in the atmosphere and space. The Administration shall provide for the widest practicable and appropriate dissemination of information concerning its activities and the results thereof."*

—NATIONAL AERONAUTICS AND SPACE ACT OF 1958

# NASA SCIENTIFIC AND TECHNICAL PUBLICATIONS

TECHNICAL REPORTS: Scientific and technical information considered important, complete, and a lasting contribution to existing knowledge.

TECHNICAL NOTES: Information less broad in scope but nevertheless of importance as a contribution to existing knowledge.

TECHNICAL MEMORANDUMS: Information receiving limited distribution because of preliminary data, security classification, or other reasons.

CONTRACTOR REPORTS: Technical information generated in connection with a NASA contract or grant and released under NASA auspices.

TECHNICAL TRANSLATIONS: Information published in a foreign language considered to merit NASA distribution in English.

TECHNICAL REPRINTS: Information derived from NASA activities and initially published in the form of journal articles.

SPECIAL PUBLICATIONS: Information derived from or of value to NASA activities but not necessarily reporting the results of individual NASA-programmed scientific efforts. Publications include conference proceedings, monographs, data compilations, handbooks, sourcebooks, and special bibliographies.

***Details on the availability of these publications may be obtained from:***

SCIENTIFIC AND TECHNICAL INFORMATION DIVISION

NATIONAL AERONAUTICS AND SPACE ADMINISTRATION

**Washington, D.C. 20546**